

Regenerator Behavior with Heat Input or Removal at Intermediate Temperatures*

Ray Radebaugh, E. D. Marquardt, J. Gary, and A. O’Gallagher

National Institute of Standards and Technology
Boulder, CO 80303

ABSTRACT

Regenerators with finite losses are capable of absorbing a limited amount of heat at intermediate temperatures along their length. This paper discusses a simple analytical model and a rigorous numerical model of regenerator behavior under the influence of heat input or heat removal at intermediate temperatures as well as the influence of a steady mass flow superimposed on the oscillating mass flow within the regenerator. The finite time-averaged enthalpy transport through the regenerator undergoes a discontinuity at the location of the heat input to satisfy the First Law of Thermodynamics. The discontinuous enthalpy flow leads to a discontinuous temperature gradient in the axial direction and to an increase in the regenerator loss that must be absorbed at the cold end. However, the increased loss is less than the heat input at the intermediate temperature, which allows the regenerator to provide a certain amount of cooling without the need for a separate expansion stage. This phenomenon is particularly useful for shield cooling and for precooling a gas continuously or at discrete regenerator locations prior to liquefaction at the cold end. For continuous precooling the total heat load can be reduced by as much as 23%.

A comparison is made of the system performance with and without intermediate heat input under various conditions. The paper presents design guidelines to determine the amount of heat a regenerator is capable of absorbing at various temperatures. Methods for optimizing the location of discrete heat inputs are presented. The analytical and numerical models are in very good agreement with each other and are consistent with very limited experimental data.

INTRODUCTION

The function of a regenerator in cryocoolers is to transfer heat from an incoming, high-pressure stream to an outgoing, low-pressure stream, just as in a recuperative heat exchanger. The only difference is that in regenerators the heat extracted from the incoming stream is stored temporarily in the heat capacity of the matrix before transferring it to the outgoing stream a short time later. Even though there are discontinuities in the flow in regenerators, there are no fundamental differences between regenerative and recuperative heat exchangers when only time-averaged behavior is considered. The finite heat capacity of a regenerator results in a

*Contribution of NIST, not subject to copyright in the U.S.

degradation of its performance, but there is no difference between the two heat exchangers in regard to their behavior under the influence of steady external factors. For example, the effect of a steady heat input along the length of a heat exchanger or a superimposed steady flow of fluid in one direction is the same for both recuperative and regenerative heat exchangers. Therefore, the arguments being presented here will apply to both types of heat exchangers, but the calculations performed here were carried out only with regenerators.

The second law of thermodynamics shows that it is always desirable to remove heat in a refrigerator at the highest possible temperature since the increase in entropy flow carried by the refrigerant to the warm end is given by

$$\Delta\dot{S} = \dot{Q} / T, \quad (1)$$

where $\Delta\dot{S}$ is the change in entropy flow, \dot{Q} is the heat input, and T is the temperature from which the heat is being input. In the case of liquefying a gas it is desirable to have many stages of cooling to remove the sensible heat from the gas and to cool it to the liquefaction temperature. The last and coldest stage only removes the heat of vaporization. In practice the additional stages may lead to a system that is too complex and costly. The simplest case is a one-stage refrigerator used to liquefy a gas like nitrogen or oxygen. For nitrogen at atmospheric pressure the specific enthalpy change from 300 K to the saturated vapor phase at 77 K is 234.0 J/g and the enthalpy change during liquefaction at 77 K is 199.2 J/g. Of the total heat that must be removed from the nitrogen, 54% should be removed at temperatures between 300 and 77 K. If this sensible heat is removed only at the single stage operating at 77 K, then system efficiency is decreased. But, with a single-stage refrigerator other heat sinks to remove some of the sensible heat at a higher temperature and improve the system efficiency are not normally available. We propose here that the heat exchanger (either recuperative or regenerative) can be used to remove a portion of the sensible heat. This concept works only with non-ideal heat exchangers as will be shown in the next section. A perfect heat exchanger cannot absorb heat along its length.

In the next sections we analyze the behavior of heat exchangers in three different cases that involve heat input (or removal) to the heat exchanger along its length. In case 1 a fixed amount of heat is input at a specific location along the length of the heat exchanger. In case 2 the heat input is proportional to the temperature change, such as with the precooling of a gas. In this case a portion of the total heat input is at some fixed location along the length of the heat exchanger and the remainder is at the cold end. Case 3 is like the previous case except that the heat is continuously removed all along the length of the heat exchanger. Case 3 also applies to the situation of a superimposed steady flow of refrigerant through the heat exchanger. In the case of regenerators this applies to the DC flow superimposed on the oscillating flow. The analysis given here applies to either sign of heat flow or to either direction of steady flow. For instance the analysis applies to the cold finger heat interceptor discussed by Johnson and Ross¹ where heat was removed at some location along the regenerator to increase the refrigeration power at the cold end. However, the emphasis in this paper is for using the regenerator or recuperator to absorb heat along its length in a manner to increase the system efficiency.

CASE 1, FIXED HEAT INPUT AT ONE LOCATION

Simple Analytical Model

For cryocooler operation above about 20 K the temperature profile in the regenerator is very near linear and the regenerator loss or energy flow (time-averaged enthalpy flow plus conduction) is approximately proportional to the temperature gradient. The contribution to the regenerator loss due to the compression and expansion of the gas in the void space is small for this temperature range. Therefore, for a simple model we assume the regenerator loss or energy flow is proportional to the temperature gradient, as given by

$$\dot{Q}_{reg} \equiv \langle \dot{H} \rangle + \dot{Q}_{cond} = -a \frac{dT}{dx} = -\dot{Q}_{reg0} \frac{LdT}{(T_h - T_c)dx}, \quad (2)$$

where $\langle \dot{H} \rangle$ is the time-averaged enthalpy flow in the regenerator (ignoring real gas effects), \dot{Q}_{cond} is the conduction in the regenerator, \dot{Q}_{reg0} is the regenerator loss or energy flow with no heat applied to the regenerator, L is the regenerator length, T_h is the temperature of the hot end, and T_c is the temperature at the cold end. Heat input along the regenerator length increases the temperature at that location so that the temperature gradient in the regenerator before and after this location is altered as shown in Fig. 1. The increased gradient at the cold end causes an increase in the regenerator loss to the cold end. The main question is whether this increased loss is less than the heat input or whether the heat input simply ends up in the cold end with no attenuation. Applying the first law of thermodynamics along the length of the regenerator shows that the new regenerator energy flow to the cold end (region 2 in Fig. 1) is given by

$$\dot{Q}_{reg2} = \dot{Q}_i + \dot{Q}_{reg1}, \quad (3)$$

where \dot{Q}_i is the heat input at some intermediate location x_i . To solve Eq. (3) for the new regenerator energy flow to the cold end, we begin by introducing the following dimensionless variables:

$$\begin{aligned} x^* &\equiv x / L \\ T^* &\equiv (T - T_c) / (T_h - T_c) \\ q_i &\equiv \dot{Q}_i / \dot{Q}_{reg0} \\ q_{reg} &\equiv \dot{Q}_{reg2} / \dot{Q}_{reg0} = - \left[\frac{dT^*}{dx^*} \right]_2 \end{aligned} \quad (4)$$

Figure 1 shows the use of dimensionless position and temperature. By using Eq. (2) and these dimensionless variables, the energy balance equation Eq. (3) can be rewritten as

$$q_{reg} = q_i - \left[\frac{dT^*}{dx^*} \right]_1, \quad (5)$$

where the last term represents the dimensionless temperature gradient in region 1. From Fig. 1 we see that the two dimensionless temperature gradients are given by

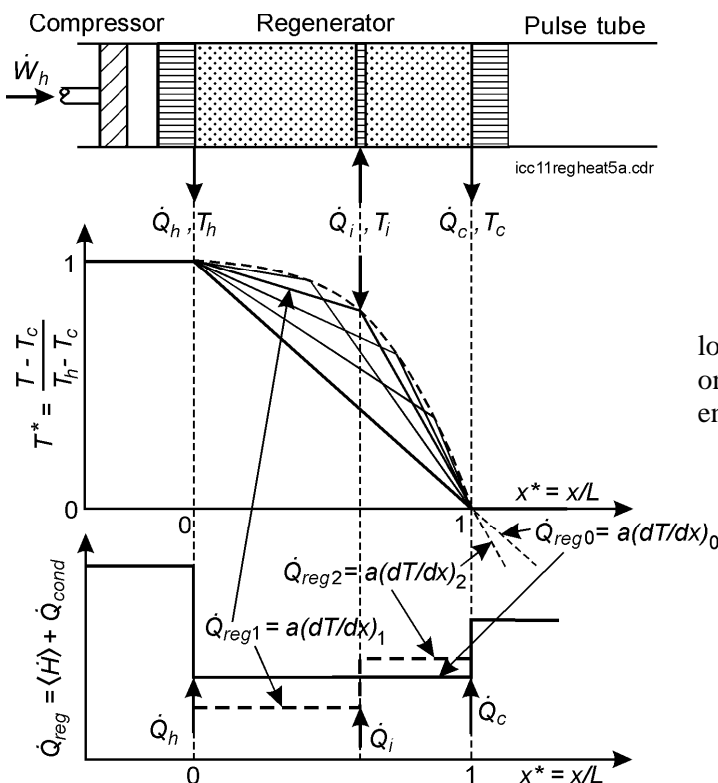


Figure 1. Diagram showing location of heat input and its effect on regenerator temperature and energy flow.

$$\left[\frac{dT^*}{dx^*} \right]_1 = \frac{T_i^* - 1}{x_i^*} = \left[\frac{x_i^* - 1}{x_i^*} \right] \left[\frac{T_i^*}{x_i^* - 1} \right] - \frac{1}{x_i^*}, \quad (6)$$

$$\left[\frac{dT^*}{dx^*} \right]_2 = -q_{reg} = \frac{T_i^*}{x_i^* - 1}, \quad (7)$$

where x_i^* is the dimensionless location for the heat input and T_i^* is the dimensionless temperature of the regenerator at that location. By substituting Eq. (7) into Eq. (6) and combining that with Eq. (5) yields

$$q_{reg} = q_i + \left[\frac{x_i^* - 1}{x_i^*} \right] q_{reg} + \frac{1}{x_i^*}. \quad (8)$$

Solving Eq. (8) for q_{reg} gives the result

$$q_{reg} = 1 + x_i^* q_i. \quad (9)$$

This equation shows that the heat input at x_i is attenuated by x_i^* and not all of the heat reaches the cold end unless $x_i^* = 1$. The ratio of the total heat load on the cold end to the heat load if the heat were input at the cold end (heat load ratio) is given by

$$q_r \equiv \frac{\dot{Q}_{reg2}}{\dot{Q}_{reg0} + \dot{Q}_i} = \frac{q_{reg}}{1 + q_i} = \frac{1 + x_i^* q_i}{1 + q_i}. \quad (10)$$

The dimensionless temperature at the location x_i^* of the heat input q_i is found by combining Eqs. (7) and (9) to give

$$T_i^* = (1 - x_i^*)(1 + x_i^* q_i). \quad (11)$$

Figure 2 shows the locus of (T_i^*, x_i^*) points for several values of q_i and Fig. 3 shows the variation of q_r with x_i^* for various q_i from Eq. (10). We note from Fig. 2 that q_i values much above 1 give rise to significant heating of the regenerator mid section. Thus, as a general statement we can say that the regenerator can be used to beneficially absorb heat along its length

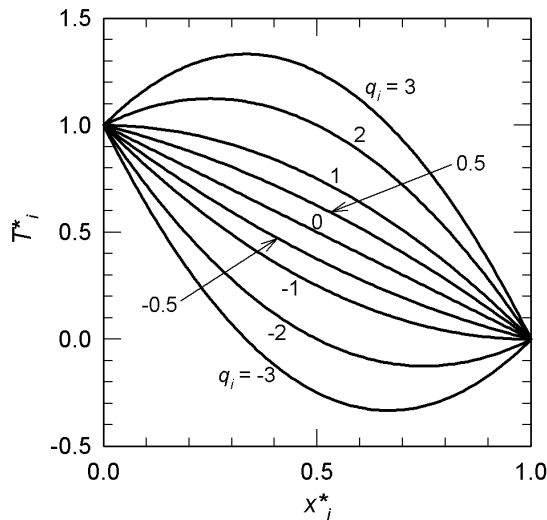


Figure 2. Dimensionless regenerator temperature at location of discrete heat input.

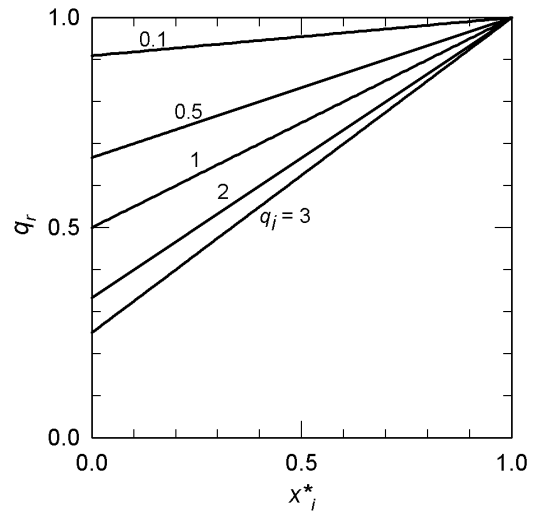


Figure 3. Heat load ratio at cold end for various heat inputs at discrete locations.

only for heat inputs not much larger than the original regenerator loss. An ideal regenerator with zero loss cannot absorb any heat along its length and the temperature at x_i would approach infinity since q_i would be infinity in Eq. (11). In simple terms, the regenerator loss in an ideal regenerator remains zero even as the temperature gradient approaches infinity. A comparison of the calculated behavior with experiment requires that \dot{Q}_{reg0} be known in order to find q_i from a known \dot{Q}_i . Typically, for 80 K cryocoolers, \dot{Q}_{reg0} is comparable to the net refrigeration power, whereas for a 60 K cryocooler \dot{Q}_{reg0} may be 50% larger than the net refrigeration power.

Numerical Model

The numerical model used here for more accurate calculations is known as REGEN3.2². It is an update of REGEN3.1^{3, 4}, which is a finite difference program using the conservation of energy, mass, and momentum equations to describe the behavior of regenerators. One of the additions in this new program is the ability to add or subtract heat at any location along the regenerator and to allow for a DC flow in either direction. The baseline case used for the calculations here was an optimized design similar to that for a pulse tube oxygen liquefier⁵. The hot and cold temperatures were 300 and 90 K. The length of the regenerator was 40 mm and it was divided into 40 cells (41 mesh points) for these calculations. The baseline regenerator loss (RGLOSS + HTFLUX in REGEN3.2) was 8.19 W. The RGLOSS term in REGEN3.2 is the total enthalpy flux minus the enthalpy flux caused by pressure changes (real gas effects). The HTFLUX term is the matrix conduction. Figure 4 compares the temperature profiles calculated from REGEN3.2 with those from the analytical model. For zero heat input there is only a slight deviation from linearity in the profile calculated by REGEN3.2. The midpoint dimensionless temperature is 0.533 compared with 0.500 for a linear profile. Heat inputs or removal were at cell midpoints and occurred at $x^*_i = 0.24$ and 0.49 . The results in Fig. 4 show that adding q_i has a greater effect on T_i in the numerical model than it does in the analytical model. For heat removal the two models agree very well.

Figure 5 compares the dimensionless regenerator loss calculated from the numerical model with that from the analytical model. This figure shows that the effect of q_i on q_{reg} is nearly the same from the two models for heat input. The largest difference in the values for q_{reg} is 0.07. For heat removal the largest difference is 0.27, which occurs with $q_i = -2.0$ at the regenerator midpoint. The temperature gradient at the cold end under those conditions is nearly zero, and the regenerator loss would be that caused by the compression and expansion in the void space. The temperature profile for heat input calculated by the analytical model would be in better

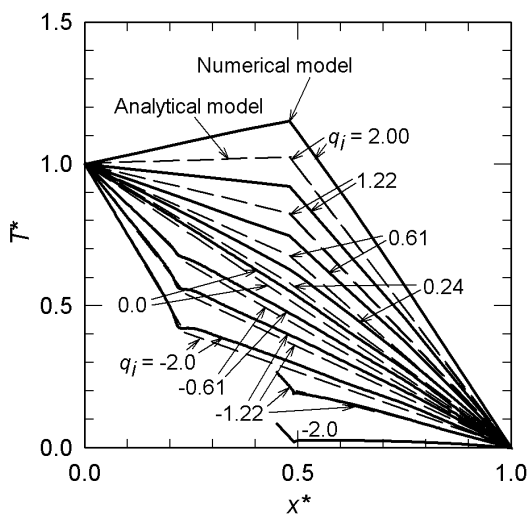


Figure 4. Dimensionless temperature profile in regenerator for various heat inputs at two different locations.

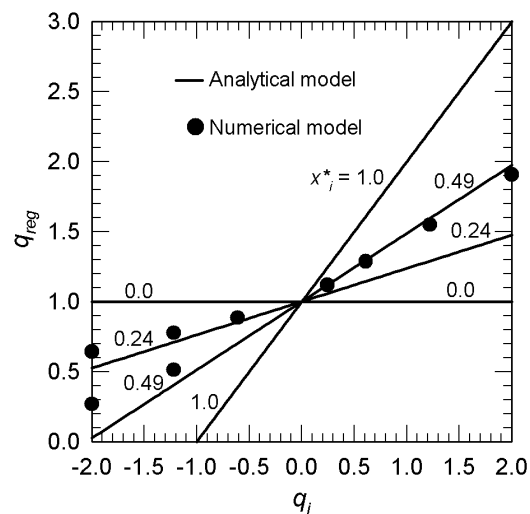


Figure 5. Dimensionless regenerator loss as a function of heat input at two different locations.

agreement with the numerical model if the compression and expansion in the void space of the regenerator were accounted for in the analytical model. That contribution is independent of the temperature gradient, which would then indicate that a constant should be added to the expressions for the regenerator loss in Eqs. (2) and (4). The dimensionless regenerator loss at any location then would be expressed as

$$q_{reg} = a\left(dT^*/dx^*\right) + b, \quad (4^*)$$

where $a + b = 1$. Equation 5 would then be changed to

$$q_i/a = \left(dT^*/dx^*\right)_1 - \left(dT^*/dx^*\right)_2. \quad (5^*)$$

By using the modified approximation to the regenerator loss given by Eq. (4*) we find that Eqs. (9) and (10) do not change, but Eq. (11) becomes

$$T_i = (1 - x_i)\left[1 + (x_i q_i / a)\right]. \quad (11^*)$$

The numerical results at $x_i = 0.49$ show that $T_i^* = 1.0$ when $q_i = 1.50$. Thus, $a = 0.77$ and $b = 0.23$ give perfect agreement with the numerical model for T_i^* at that value of q_i and deviates only by 0.03 at $q_i = 0$. At $q_i = -2.0$ for the midpoint we found that $q_{reg} = 0.27$ when the temperature gradient at the cold end went to zero. That value agrees well with $b = 0.23$. However, the results for T_i^* from the numerical model for heat removal agree very well with the analytical model when $b = 0$. To maintain simplicity in the remaining sections, we will consider only the case of $a = 1.0$ and $b = 0$. Such an approximation is reasonably good for a first stage regenerator, but a second stage regenerator will have a rather large b and require the use of the modified analytical model. For temperatures below about 20 K the regenerator temperature profile with zero heat input to the regenerator begins to deviate considerably from linearity with a dimensionless temperature at the center point being much less than 0.5. Thus, we do not expect that the analytical model would be useful for temperature below about 20 K.

Figures 4 and 5 show that when heat is removed at $x_i^* = 0.24$ to a heat sink at about 180 K ($T_i^* = 0.43$), the regenerator loss can be reduced by 36%. For the case of regenerator loss being comparable to the net refrigeration power, the heat intercept leads to an increase in net refrigeration of 36% for the same power input or a reduction in input power by 36% for the same net refrigeration power. These calculated improvements are consistent with that found experimentally by Johnson and Ross¹ with a Stirling cryocooler when a heat interceptor at 150 K increased the net cooling power at 60 K by 30%.

CASE 2, TEMPERATURE DEPENDENT HEAT INPUT

We now consider the case where the regenerator is used to precool a gas. The amount of heat flow at a particular location along the regenerator depends on the temperature difference between the hot end temperature and the temperature at the specified location on the regenerator. The gas is cooled the rest of the way to the cold temperature by the refrigeration power available at the cold end. In this case we still consider only one heat sink located along the regenerator. The following section deals with a continuous heat transfer along the entire length.

The total heat that must be removed by the regenerator and the cold end for this case is given by

$$\dot{Q}_t = \alpha(T_h - T_c), \quad (12)$$

where $\alpha = \dot{m}C_p$ for the case of fluid flow at a mass flow rate of \dot{m} with a constant specific heat of C_p . The heat flow into the regenerator at the temperature T_i is

$$Q_i = \alpha(T_h - T_i) \quad (13)$$

and the heat flow into the cold end becomes

$$\dot{Q}_c = \alpha(T_i - T_c). \quad (14)$$

The sum of the heat flows into the cold end when the regenerator loss is considered is

$$\dot{Q}_{sum} = \dot{Q}_{reg2} + \dot{Q}_c, \quad (15)$$

which, when normalized by the baseline regenerator loss \dot{Q}_{reg0} becomes

$$q_{sum} = q_{reg} + q_c. \quad (16)$$

Because T_i is not known at this time, the only heat flow known at this time is \dot{Q}_t from Eq. (12). When it is normalized by \dot{Q}_{reg0} it becomes q_t . The other two heat flows are related to q_t in the following manner:

$$\begin{aligned} q_i &= q_t(1 - T_i^*) \\ q_c &= q_t T_i^*. \end{aligned} \quad (17)$$

We now solve for T_i^* in terms of the known quantities x_i^* and q_t . Substituting q_i from Eq. (17) into Eq. (11) allows us to write T_i^* as

$$T_i^* = (1 - x_i^*) \left[1 + x_i^* q_t (1 - T_i^*) \right]. \quad (18)$$

The solution for T_i^* at any x_i^* for various q_t becomes

$$T_i^* = \frac{(1 - x_i^*)(1 + x_i^* q_t)}{1 + x_i^* q_t (1 - x_i^*)}. \quad (19)$$

The sum of heat flows to the cold end is found by substituting Eqs. (17) and (9) into Eq. (16), which yields

$$q_{sum} = 1 + x_i^* q_t (1 - T_i^*) + q_t T_i^*. \quad (20)$$

The ratio of this heat flow to the heat flow at the cold end if all the heat was delivered to the cold end is

$$q_r = \frac{\dot{Q}_{sum}}{\dot{Q}_{reg0} + \dot{Q}_t} = \frac{q_{sum}}{1 + q_t}. \quad (21)$$

Figures 6 and 7 show how T_i^* and q_r vary with x_i^* for different values of q_t from the simple analytical model. For all q_t the optimum location for the heat intercept is at the midpoint of the regenerator. The minimum q_r is 0.889, which occurs with $q_t = 2.0$. The value of T_i^* at the midpoint with this heat input is 0.667, which means that 1/3 of the heat is transferred to the regenerator and 2/3 is transferred to the cold end. Thus, the use of the regenerator to precool a gas can reduce the total heat load on the cold end by up to 11%. It should be pointed out that the baseline heat load considered here includes the baseline regenerator loss as well as the net heat load of cooling the gas from the warm temperature to the cold temperature. If the regenerator loss were equal to the net refrigeration power, then precooling at the midpoint would reduce the required net refrigeration by up to 22% at the optimum condition.

CASE 3, CONTINUOUS HEAT TRANSFER (GAS PRECOOLING)

Analytical Model

The most efficient use of the regenerator to precool a gas or a conduction member is with continuous heat transfer all along the length of the regenerator. The first law of thermodynamics

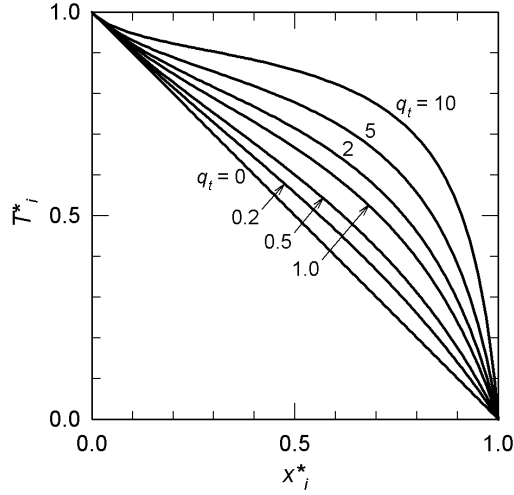


Figure 6. Dimensionless temperature at location of single heat sink for various total heat inputs.

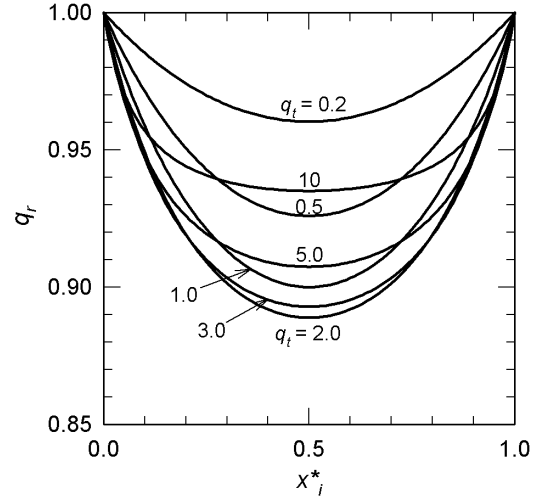


Figure 7. Heat load ratio at cold end versus heat sink location for various total heat inputs.

applied to an infinitesimally small element shows that the regenerator energy flow at any location, given by Eq. (2), undergoes a change given by

$$\frac{d\dot{Q}_{reg}}{dx} = -\frac{d\dot{Q}}{dx}, \quad (22)$$

where \dot{Q} is the heat flow caused by changing the temperature of a gas. In accordance with Eq. (12) this heat flow is represented by $d\dot{Q} = \alpha dT$. By using the linear assumption in Eq. (2) for the regenerator, Eq. (22) becomes

$$a \frac{dT^2}{dx^2} = \alpha \frac{dT}{dx}. \quad (23)$$

Equation (23) can be written in dimensionless quantities as

$$\frac{d^2 T^*}{dx^{*2}} = q_t \frac{dT^*}{dx^*}. \quad (24)$$

The solution to Eq. (24) gives the dimensionless temperature profile along the regenerator as

$$T^* = \frac{e^{q_t x^*} - e^{q_t}}{1 - e^{q_t}}. \quad (25)$$

Figure 8 shows the dimensionless temperature profile for various q_t . The dimensionless regenerator loss or energy flow at any location with this additional heat input to the regenerator according to Eq. (4) is given by

$$q_{reg} = -\frac{dT^*}{dx^*} = -\frac{q_t e^{q_t x^*}}{1 - e^{q_t}}. \quad (26)$$

Figure 9 shows this regenerator energy flow along the regenerator for various q_t . The ratio of the total heat flow to the cold end when using the regenerator for precooling to that without the precooling is given by

$$q_r = \frac{\dot{Q}_{reg2}}{\dot{Q}_{reg0} + \dot{Q}_t} = \frac{q_{reg}(x^* = 1)}{1 + q_t} = -\frac{q_t e^{q_t}}{(1 + q_t)(1 - e^{q_t})}. \quad (27)$$

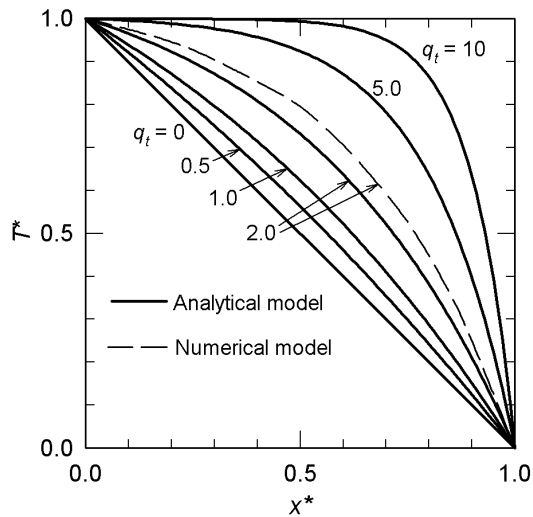


Figure 8. Dimensionless temperature profile in regenerator for continuous heat input or steady mass flow toward cold end.

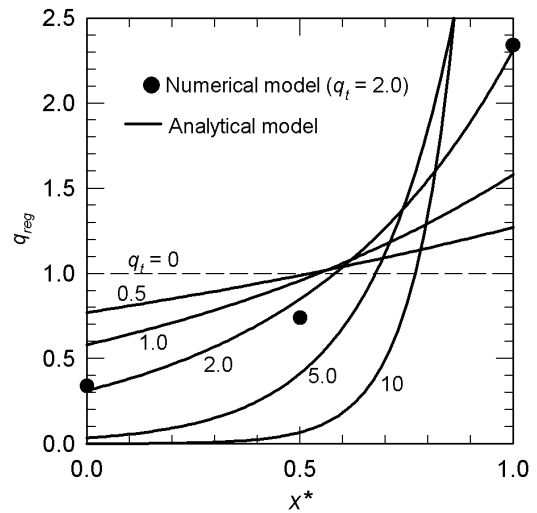


Figure 9. Dimensionless regenerator energy flow versus position in regenerator for continuous heat input or steady mass flow.

A graph of q_r is shown in Fig. 10 and is discussed in the following section where it is compared with the results from the numerical model. The minimum q_r of 0.770 occurs at $q_t = 1.80$. Thus, the continuous heat transfer can reduce the total heat load (including baseline regenerator loss) on the cold end by a maximum of 23%.

Numerical Model (with steady mass flow)

The REGEN3.2 numerical model can be used to simulate continuous heat transfer to the regenerator by superimposing a steady or DC mass flow on the oscillating flow. When simulating the precooling of any gas other than helium, the steady mass flow rate of helium in REGEN3.2 needs to be adjusted to give the same enthalpy change between the hot and cold temperatures as for the gas to be precooling. We are assuming that the specific heats of both gases are independent of temperature. Starting with the same baseline case discussed for Case 1, we ran REGEN3.2 for three different steady mass flows which simulated total dimensionless heat flows from the hot to the cold end of $q_t = 0.5, 2.0,$ and 5.0 . The calculated temperature profile for the case of $q_t = 2.0$ is shown in Fig. 8. The numerical model shows slightly higher temperature sensitivity than does the analytical model, Eq. (25). As discussed previously, the

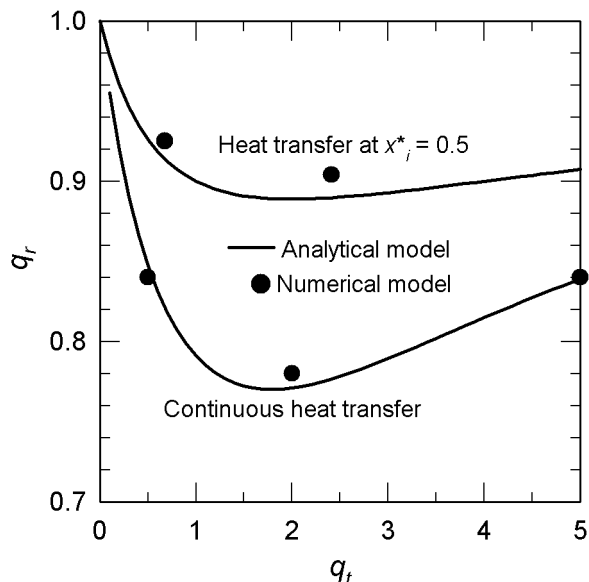


Figure 10. Heat flow ratio to cold end with heat transfer at the optimum discrete location ($x^*_i = 0.5$) and with continuous heat transfer or steady mass flow.

difference can be explained by the neglect in the analytical model of a contribution due to compression and expansion in the void space. The regenerator energy flow calculated with the numerical model for the case of $q_t = 2.0$ is compared with that from the analytical model in Fig. 9. Results from the two models agree very well, particularly at the two ends of the regenerator. Values of q_{reg} much greater than about 2 or 3 would tend to reduce the net refrigeration power to zero for cryocoolers operating around 80 K. Figure 10 compares the heat flow ratio q_r of Eqs. (10) and (27) for the analytical model with that obtained from REGEN3.2. This figure shows that the continuous heat transfer significantly reduces the cold end heat load compared with the case of heat transfer only at the midpoint. The numerical and analytical models agree well for both discrete and continuous heat inputs.

COMPARISON WITH EXPERIMENT

Gilman⁶ shows that with a heat intercept strap at a location of $x_i^* = 0.25$ with $T_i^* = 0.458$ the cooling power increased from 1.65 W to 2.40 W, or a 45% gain at 60 W input power. From Eq. (11) we find that $q_i = -1.56$ and from Eq. (9) we find that $q_{reg} = 0.61$, or a 39% reduction in the regenerator loss. The radiator load from Gilman's results was 3.1 W, which for a $q_i = -1.56$ gives a baseline regenerator loss of 1.99W. A 39% reduction of this loss would cause a 0.78 W increase in refrigeration power compared with Gilman's measured result of 0.75 W. Our numerical model would predict a gain of about 0.62 W and agrees to within about 17% of the experimental result. Our experimental results with liquefaction of nitrogen⁷ showed an increased liquefaction rate of 17% when the incoming gas was continuously precooled by the outer surface of the regenerator. The ratio of sensible heat of nitrogen to the heat of vaporization is 1.18. In this example the refrigeration power is comparable to the regenerator loss, and the calculated results from Fig. 10 show a predicted increased liquefaction rate of about 22%.

CONCLUSIONS

A simple analytical model has been developed that can be used to calculate the effect of heat input or removal along the length of a regenerator. The model assumes a linear temperature profile in the regenerator, which is a good approximation for temperatures down to about 20 K. The model is also extended to the case of continuous heat transfer all along the length of the regenerator and to a steady mass flow superimposed on the oscillating flow. The analytical model is in good agreement with our most recent numerical model, REGEN3.2. For continuous precooling in gas liquefaction, the heat load can be reduced by up to 23%. The calculated results are in reasonable agreement with experiments using heat interceptor straps and with those obtained in the liquefaction of nitrogen with a pulse tube refrigerator.

REFERENCES

1. Johnson, D. L., and Ross, R. G., Jr., "Cryocooler Coldfinger Heat Interceptor", *Cryocoolers 8*, Plenum Press, New York (1995), pp. 709-717.
2. Gary, J., O'Gallagher, A., Radebaugh, R., and Marquardt, E., "REGEN3.2 Regenerator Model: User Manual", NIST Technical Note, to be published.
3. Gary, J., Daney, D. E., and Radebaugh, R., "A Computational Model for a Regenerator", Proc. Third Cryocooler Conf., NIST Special Publication 698 (1985) pp. 199-211.
4. Gary, J., and Radebaugh, R., "An Improved Model for Calculation of Regenerator Performance (REGEN3.1)", Proc. Fourth Interagency Meeting on Cryocoolers, David Taylor Research Center Technical Report DTRC-91/003 January 1991, pp. 165-176.
5. Marquardt, E. D., and Radebaugh, R., "Pulse Tube Oxygen Liquefier", *Adv. Cryogenic Engineering*, vol. 45, Plenum Press, New York (2000), in press.
6. Gilman, D. C., "Cryocooler Heat Interceptor Test for the SMTS Program", *Cryocoolers 9*, Plenum Press, New York (1997), pp. 783-793.
7. Marquardt, E. D., Radebaugh, R., and Peskin, A. P., "Vapor Precooling in a Pulse Tube Liquefier", *Cryocoolers 11*, Plenum Press, New York (2001), in press.